PCCP

Accepted Manuscript

ROYAL SOCIETY OF CHEMISTRY

www.rsc.org/pccp

Journal Name

ARTICLE

Triarylborane conjugated dicyanovinyl chromophores: Intriguing Optical properties and colorimetric anion discrimination

Received 00th January 20xx,
Accepted 00th January 20xx

DOI: 10.1039/x0xx00000x

www.rsc.org/

George Rajendra kumar, Samir Kumar Sarkar and Pakkirisamy Thilagar*

Three new triarylborane conjugated dicyanovinyl chromophores (Mes_2B-π-Donor-DCV; donor: N-methyldiphenylamine (**1**) and triphenylamine (**2** and **3** [with two $BMes_2$ substitutions]) of type A-D-A (acceptor-donor-acceptor) are reported. Compounds **1**-**3** exhibit intense charge transfer (CT) absorption bands in visible region. These absorption peaks are combination CT bands of both amine donor to $BMes_2$ and donor to DCV units. This inference was supported by theoretical studies. Compound **1** show weak fluorescence compared to **2** and **3.** Discrimination of fluoride and cyanide ions is essential in the case of triarylborane (TAB) based anion sensors as they give similar response towards both the anions. Anion binding studies of **1**, **2** and **3** showed that, fluoride ions binds selectively to the boron centre and blocks the corresponding CT transition (donor to $BMes_2$) leaves another CT transition to be red shifted. On the other hand, cyanide ions bind with both the receptor cites and stops both the CT transition process and hence different colorimetric response was noted. The binding of F^-/CN^- induce colour changes in the visible region of the electronic spectra of **2** and **3**, which allows naked-eye detection of F^- and CN^- ions. Anion binding mechanisms are established using NMR titration experients.

Introduction

Owing to their intriguing optical properties, Triarylborane (TAB) containing functional luminescent molecules have attracted a lot of attention of materials chemist. Presence of empty p orbital on boron atom and its effective electronic communication with the attached aromatic π electron units makes these molecular systems as potential candidates for modern materials[1] such as OLED (organic light emitting diodes) materials[2], NLO devises[3], luminescent polymers[4] and sensor[5]. It has been well demonstrated over the past fifteen years that, TABs can selectively bind with fluoride (essential and at the same time toxic if it is in excess) and cyanide ions (an important anion in most of the industrial processes but toxic towards biosphere). The binding of F^-/CN^- to the Lewis acidic boron centre modify the optical properties of TABs by perturbing the electronic communication between boron and attached π-systems.[5a, i] Since, the binding event of both the anions F^- and CN^- follow the same route (interrupting conjugation between B and π-systems), TABs exhibit similar optical response for these anions. Thus, anions F^- and CN^- are called interfering anions in TAB based sensor chemistry.

Recently, we become interested in sensors chemistry, by exploiting the excited state energy transfer process and we have developed a series of anion sensors. [6] Many research groups are focused on sensing Fluoride and Cyanide ions as the two anions have beneficial as well as detrimental effects. [7] As part of on-going program, we intended to develop boron based sensor which can discriminate interfering anions such as fluoride and cyanide. Very recently we have successfully demonstrated differential identification of fluoride and cyanide ions using a TAB-phorphyrin-Zn conjugate (chart I 1.1).[8a] Presence of two dissimilar Lewis acidic receptor sites enabled us to identify the interfering anions with different optical behaviours. The complexity in the molecular design prompted us to simplify the design principle for the said application, and subsequently we have developed a TAB-dicyanovinyl (DCV) conjugate (Chart 1: 1.2 and 1.3)[8b]. The sterically less hindered boron centre in 1.2 prefers to coordinate with both F^- and CN^-, while the sterically more hindered boron in 1.3 prefers to bind selectively with fluoride over cyanide ions. Consequently in 1.3, fluoride interacts with boron centre and cyanide with electrophillic carbon centre of DCV unit and thereby gives different optical outputs for these two anions. Using similar design strategy, very recently Zhao et all developed TAB-DCV conjugate (Chart 1: 1.4) for the selective discrimination of fluoride and cyanide ions. [8c]

[a] *Inorganic and Physical Chemistry department, Indian Institute of Science, Bangalore-560012, India. E-mail: thilagar@ipc.iisc.ernet.in*

†Electronic Supplementary Information (ESI) available: [NMR spectra, crystal and DFT data, calculation of binding constant and detection limit]. CCDC numbers corresponding to crystals **1** and **2**: 1052590 and 1417197 See DOI: 10.1039/x0xx00000x

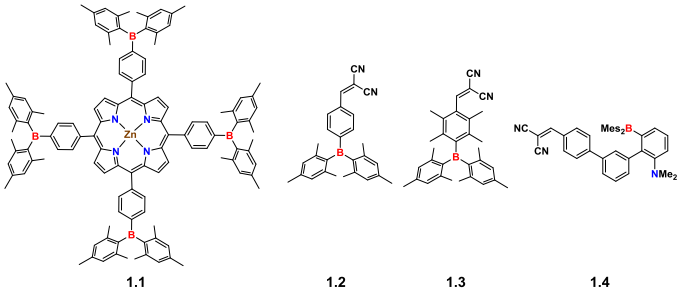

Chart I: Molecules reported in previous works

It has been well established that, with a suitable electron rich amine attached, the electron deficient boryl unit show an intermolecular charge transfer character.[9] Very recently, we demonstrated that attachment of two different acceptor units on a single donor (triphenylamine) exhibited two dissimilar ICT bands in the visible region of the electronic spectra. We envisioned that if two different electron deficient receptors such as TAB and DCV units are attached with a suitable amine donor would exhibit two distinct ICT bands in the electronic spectrum.[10] We also proposed that if the two ICT process occurred in the visible region of the electronic spectra, the presence of two different receptors would be conveniently exploited for the naked-eye discrimination of additional opportunity to selectively exploit the two ICT process for the discrimination of different anions. To verify our hypothesis, we designed and synthesised compounds **1**, **2** and **3**, incorporating DCV, -$BMes_2$ and amine (TPA/ units (Chart II). Our anticipation is realised with compounds **2** and **3** and the results are reported in this paper.

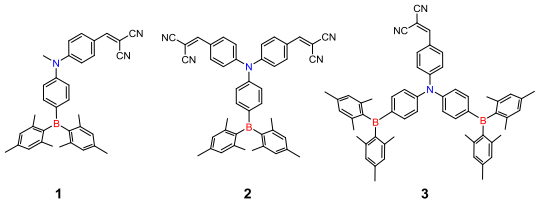

Chart II: Molecules under investigation in present work.

Results and discussion

Synthesis and Characterisation:

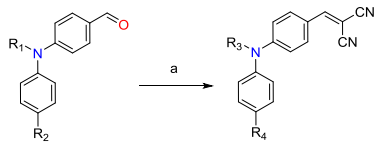

1.1: R_1 = -CH_3 & R_2 = -$BMes_2$
2.1: R_1 = -Ph-CHO & R_2 = -$BMes_2$
3.1: R_1 = -Ph-$BMes_2$ & R_2 = -BMes2

1: R_3 = -CH_3 & R_4 = -$BMes_2$
2: R_3 = -Ph-$CH(CN)_2$ & R_4 = -$BMes_2$
3: R_3 = -Ph-$BMes_2$ & R_4 = -BMes2

Scheme 1: a) $CH_2(CN)_2$, piperidene, ethanol/DCM

Synthetic schemes for the preparation of precursors are given in the supporting information (Scheme S1). Formylation of **A** using n-BuLi and DMF gave **B** in good yield. The aldehyde group in **B** was converted into acetal by refluxing it with triethylorthoformate in the presence of a catalytic amount of HCl in ethanol followed by borylation using n-BuLi and dimesitylfluoroborane ($BFMes_2$) yielded **1.1**. Compounds **2.1** and **3.1** are prepared by adopting the procedure reported by us recently.[10] Compounds **1**, **2** and **3** are prepared by base (piperidine) catalysed condensation of respective aldehydes (**1.1** for **1**, **2.1** for **2** and **3.1** for **3)** with required amount of malanonitrile (0.07 mL for **1**, 0.029 mL for **2** and 0.021 mL for **3**) in the mixture of ethanol and dichloromethane solvents (scheme1). All the compounds are characterised by ^1H, ^{13}C NMR spectroscopy, HRMS mass spectrometry. Compounds **1** and **2** are structurally characterised by single crystal X-ray diffraction studies.

Molecular structure of 1 and 2

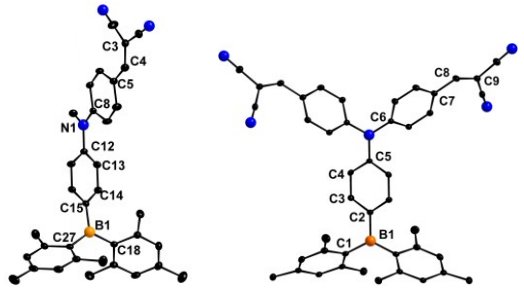

Figure 1: Molecular Structure of **1** (left) and **2** (right). Blue = nitrogen, black = carbon, orange = boron.

The molecular structures of **1** and **2** are shown in Fig. 1 (see ESI for structure refinement details[11] and Table 1 for selected bond lengths). The tricoordinated boron centre adopts a trigonal planar geometry which is typical of sp^2 hybridized boron.[5a & 10] The nitrogen centre in TPA and DPA moieties also adopted trigonal planar geometry. The phenyl ring which connects $BMes_2$ and NPh_2 unit in **2** is in quinonoid form which imparts the evidence for the presence of strong electronic conjugation between the boryl acceptor and amine donor. The torsional angle between the TAB plane (BCC) and TPA/DPA plane (NCC) is 86.7° and 21.6° for **1** and **2** respectively. The dihedral angle between BCC and phenyl ring found in **1** (25.29°) is significantly higher than the value found in **2** (19.43°). The dihedral angle between the phenyl unit and NCC are also following the similar trend (62.40° and 40.58° for **1** and respectively **2)**. Based on these results one can tentatively conclude that the donor acceptor interactions in **1** are weaker than in **2**. In both the compounds the DCV unit and its neighbouring phenyl ring are adopted coplanar arrangement. These results clearly indicate that there could be significant electronic conjugation between donor (amine) and acceptor (Boryl/DCV) units.

Optical Properties:

The electronic spectra of compounds **1-3**, **TPA-$BMes_2$** and **TPA-DCV** are shown in figure 2 and 3 respectively. The absorption bands of all the compounds fall in the visible region (~450 nm) (Figure 2 and Table 2). Compound **1** exhibits two absorption bands at ~344 and 440 nm. Compounds **2** (336, 416 and 476 nm) and **3** (330, 386 and 462 nm) exhibit three

Table 1. Selected bond lengths noted in molecular structures of **1** and **2**

Molecules	Bond Length (Å)								
1	B1-C1	B1-C2	N1-C5	N1-C6	C2-C3	C3-C4	C4-C5	C7-C8	C8-C9
	1.576	1.570	1.430	1.417	1.410(4)	1.388	1.395	1.450(4)	1.352(4)
2	B1-C15	B1-C18	N1-C12	N1-C8	C12-C13	C13-C14	C14-C15	C3-C4	C4-C5
	1.564(4)	1.573(4)	1.435(3)	1.367(3)	1.402(5)	1.380(4)	1.391(4)	1.401(4)	1.404(4)

absorption peaks in the region 330 to 480 nm. In compounds **1-3**, the intensity of lower energy bands are significantly stronger than the higher energy bands. The higher energy band observed at ~ 335 nm in **1-3** can be ascribed to the π-π* transitions involved in aryl groups in amine donor as well as the triarylborane unit. The lower energy bands observed for **1-3** in the region ~380-475 are ascribed to the combined intramolecular charge transfer (ICT) transition of donor amine to boryl acceptor and donor amine to acceptor DCV units. The lower energy transitions observed for **2** is significantly red shifted compared to **1** and **3**. This can be attributable to the extended π-conjugation due to the presence of additional vinyl unit in **2**. As hypothesized vide-supra, the presence of two dissimilar acceptors boryl and DCV units invoked two distinct ICT process at different energy regions of electronic spectra of **2** and **3**. This absorption features are completely different from the observations noted for model compounds **DCV-TPA** and **TPA-BMes$_2$.** To gain further insight into the absorption features of **1-3**, their optical spectra were recorded in solvents with different polarity (Figure 4-6). The higher energy band in the region ~335 nm was not perturbed by solvent polarity. However, the lower energy bands of **1-3** significantly red shifted when increasing the solvent polarity from hexane to dimethylsulphoxide (**1**: 418 to 447 nm, for **2**, 403 to 420 nm and 458 to 478 nm and for **3:** 381 to 392 nm and 449 to 466 nm). These results clearly indicate that the lower energy bands have charge transfer character, which is in line with our above inference.

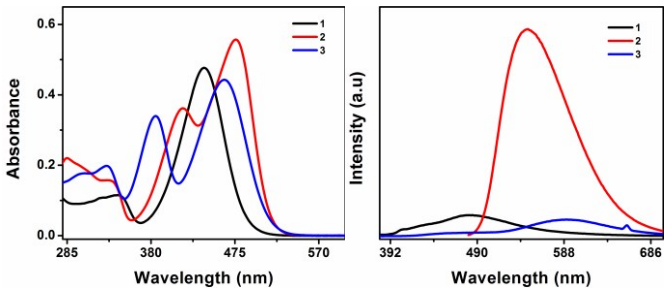

Figure 2: UV-Vis absorption (left) and Fluorescence (right) spectra of compounds **1** (λ_{ex} = 340 nm), **2** (λ_{ex} = 416 nm), and **3** (λ_{ex} = 330 nm) in dichloromethane (1×10^{-5} M).

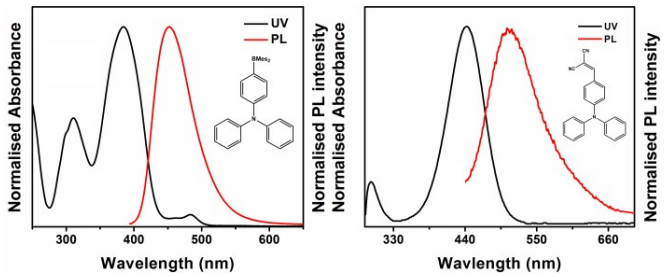

Figure 3: UV-Vis absorption and fluorescence spectra of model compounds.

Upon excitation at 350 nm, **2** exhibit single emission band at ~546 nm, while dual emission bands were observed for **1** (~481 nm and ~590 nm) and **3** (at ~460 and 593 nm). The fluorescence quantum yield of **2** is significantly higher than that calculated for **1** and **3**. The time resolved fluorescence studies clearly indicate that the non radiative process is prominent in **1** compared to **2** and **3** (table 2). The dissimilarities in the radiative and non-radiative decay constants (K_r and K_{nr}) of **1**, **2** and **3** can be attributable to the difference in their molecular rigidity. The presence of additional boryl unit in **3** resulted in lowering K_r value and hence shows slightly lower quantum yield compared to **2** and is in line with the literature report.[3e] The excitation spectra of **2** nearly reproduced the absorption

Table 2. Optical properties of **1-3** in dichloromethane (1×10^{-5} M)

Compounds	λ_{abs} (nm)	λ_{em} (nm)	Φ_F [a](%)	τ (ns)	K_r (1×10^6 S^{-1})[b]	K_{nr} (1×10^8 S^{-1})[b]
1	344, 440	481	1.03	4.59	2.24	2.16
2	336, 416, 476	546	14.92	19.27	7.74	0.44
3	330, 386, 462	460, 592	4.71	14.70	3.2	0.64

[a]Absolute quantum yields are measured using integrating sphere; [b]K_r - radiative decay constant, K_{nr} – non-radiative decay constant [calculated using the relationship, $K_r = \Phi/\tau$ & $K_{nr} = (1-\Phi)/\tau$]

spectra, which indicate that all the states are equally contributed to the emission process. The excitation spectra of corresponding emission peaks in dual emissive compounds **1** and **3**, indicate that the higher energy emission band is mostly boryl based while the lower energy band has the contribution from both boryl and DCV based ICT states (ESI. Figure S11-S13).

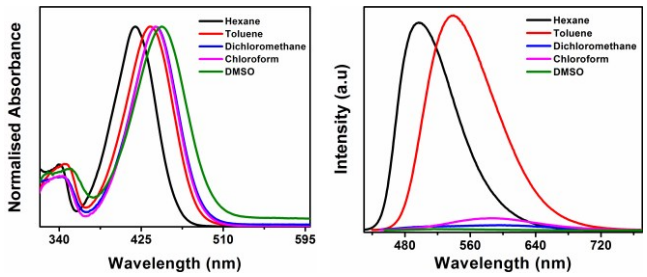

Figure 4: Solvent dependent UV-Vis absorption (left) and Fluorescence (right) spectra of **1** (1×10^{-5} M).

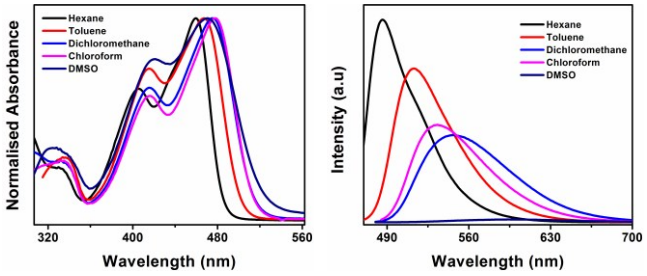

Figure 5: Solvent dependent UV-Vis absorption (left) and Fluorescence (right) spectra of **2** (1×10^{-5} M).

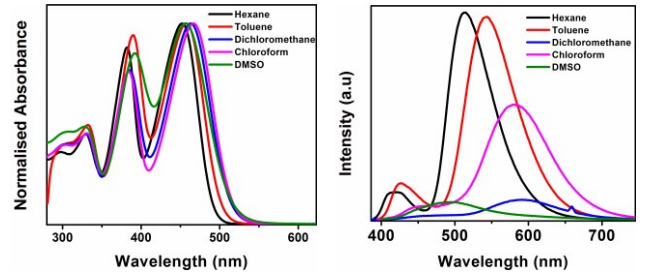

Figure 6: Solvent dependent UV-Vis absorption (left) and Fluorescence (right) spectra of **3** (1×10^{-5} M). When polarity of the environment increased, changes in photo physical properties are noted.

Solvatofluorochromic behaviour of **1**, **2** and **3** were studied. In all the cases, as the solvent polarity increases, the emission band undergoes red shift with decreasing intensity. These observations are typical of a D-A systems. Upon excitation at 420 nm, **1** shows a single emission band at ~480 nm ($\Delta\nu$ = 2976 cm^{-1}) in hexane, in DCM red shifted to ~600 nm ($\Delta\nu$ = 7142 cm^{-1}) and in DMSO negligible fluorescence was observed (Fig. 4). Probably the charge separated excited state is stabilised to more extent and prefers to relax only via non radiative decay pathway in polar environment. Similarly, the emission bands of **2** and **3** also bathochromically shifted in polar solvents (Figure 5). When changing the solvent from hexane to DMSO, compound **2** show a 110 nm red shift ($\Delta\nu$ = 3420 cm^{-1} and 7232 cm^{-1} in hexane and DMSO respectively) while compound **3** showed 87 nm redshift ($\Delta\nu$ = 5439 cm^{-1} and $\Delta\nu$ = 9794 cm^{-1} in hexane and DMSO, respectively) (Figure. 6). The observed higher Stokes shift in polar solvents clearly indicates that the polar ICT emissive states operative in **1, 2** and **3**.

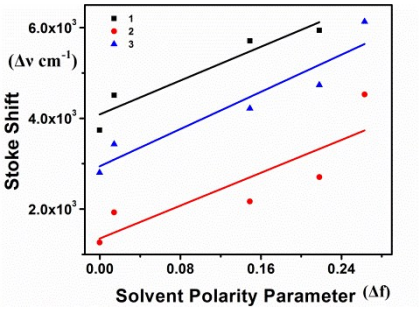

Figure 7: Lippert Mataga plots for compounds **1-3**. A linear relationship is noted between stokes shift and solvent polarity parameter.

To rationalise the higher Stokes shift observed for **1-3**, in polar solvents, Lippert-Mattaga plots[12] were derived using the relationship between solvent polarity paramenter and stokes shift (Figure. 7). Using the formula, $\Delta f = [(D-1)/(2D+1)] - [(n^2-1)/(2n^2+1)]$ and $\Delta\nu = (\nu_A-\nu_F)$ $cm^{-1} = (2\Delta\mu^2/hca^3)\,\Delta f$ + Constant, where D and n represents dielectric constant and refractive index of a solvent, $\Delta\mu$ is change in dipolemoment [$\Delta\mu = \mu_g - \mu_e$, μ_g and μ_e are dipolemoment in ground and excited states respectively. h Plank's Constant, c velocity of light and a Onsagar radius. All the compounds show linear relationship between $\Delta\nu$ and Δf. The calculated change in dipole moments ($\Delta\mu$) of **1** (~27D), **2** (~26D) and **3** (~28D) directly support our above inference regarding higher Stokes shift in polar environments.

Theoretical Investigations:

To gain further insight into the electronic structure of compounds **1**, **2**, and **3**, DFT computational studies were performed [13] using the B3LYP functional and 6-31G(d) as basis set. The frontier molecular orbitals of compounds **1-3** are depicted in Figure. 8

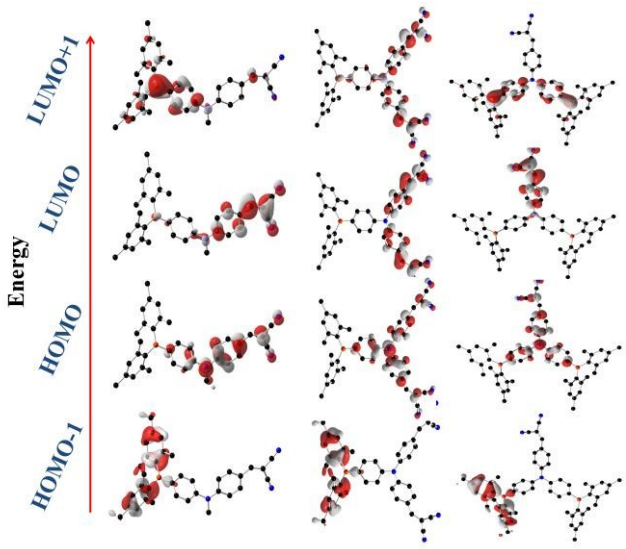

Figure 8: The frontier molecular orbitals for **1**, **2**, and **3** (isovalue = 0.04). Hydrogen atoms are omitted for clarity.

Molecular orbital (MO) coefficients of HOMO-1 of compounds **1-3** are localised on the π orbital of mesityl ring with significant contribution from B-C (C_6H_4 of amine donor) σ-bond. HOMO is mainly concentrated on amine with considerable contribution from DCV units. The LUMO are largely centred on DCV unit with considerable contribution from the phenyl spacer which connects the DCV with N centre. The LUMO+1 is mostly concentrated on empty p-orbital on boron centre with effective contribution from the C_6H_4 which connect it with N centre (Figure. 8). These results clearly indicate the presence of electronic communication between the donor amine and acceptor TAB and DCV moieties. The possible electronic transitions involved in **1-3** were calculated using TD-DFT method. Theoretically predicted electronic spectra of **1-3** are in close agreement with experimentally observed values. In the case of compound **1**, the calculated transition at 406 nm is primarily from HOMO to LUMO transition. Thus the lower energy transition noted in the absorption spectrum of **1** is mainly due to the CT transition from DPA (diphenylamine) to the DCV unit. Calculated transitions of **2 (**467 nm and 422 nm) and **3** (449 nm and 400 nm) are arising from HOMO→LUMO and HOMO→LUMO+1 respectively. These results directly support our assumptions of experimentally observed UV-Vis absorption peaks for **2 (**~476 and ~416 nm) and **3** (~462 and ~386 nm) as TPA→DCV and TPA→TAB charge transfer transitions respectively.

Anion Binding Studies

To evaluate the anion sensing abilities of compounds **1-3**, these compounds were titrated against various anions such as fluoride, chloride, bromide, iodide, nitrate, hexa fluoro phosphate, perchlorate, acetate, hydrogen phosphate and cyanide. The changes associated with the optical properties of **1-3** in the presence of anions were monitored by using UV-Vis and fluorescence spectrometer. The results show that compounds **1-3** selectively binding to fluoride and cyanide and show distinct colour changes for these two anions (ESI, Figure S27).

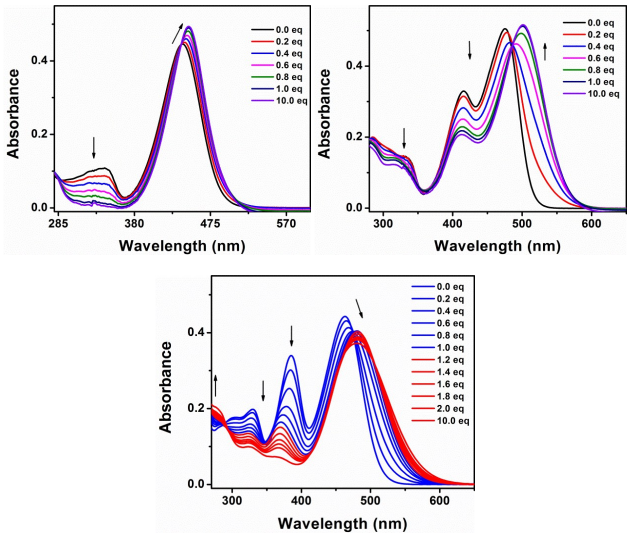

Figure 9: Changes in UV-Vis-absorption spectra of **1** (1 × 10^{-5} M, top left), **2** (1 × 10^{-5} M, top right) and **3** (1 × 10^{-5} M, bottom) in presence of TBAF (2 μL = 1 eq) in dichloromethane. Boryl based absorption is decreased, while CT band ~440, 476 and 460 nm undergoes red shift.

Fluoride binding in **1**, **2** and **3** decrease the intensity of band(s) at ~340 (for **1**), ~ 340 nm and 415 nm (for **2**) and 330 and 386 nm (for **3**) respectively (Figure. 9). The intensity of lower energy bands of **1** and **2** (440 nm and 476 nm) increased with bathochromic shift in the presence of fluoride. In contrast, the intensity of the lower energy band (460 nm) in **3** decreases with bathochromic shifts when binding with fluoride. The bathochromic shift observed for **2** (33 nm) and **3** (20 nm) are significantly higher than the value observed for **1** (9 nm). Fluoride binding changes the Lewis acidic TAB unit to electron rich borate moiety; consequently the electronic and structural changes in the individual moiety facilitate the $Ar_3BF^- \rightarrow$ DCV intermolecular charge transfer. As envisioned vide-supra, in the case of **2** and **3**, the bathochromic shit associated with a distinct colour change from 476 to 509 nm and 460 to 480 nm respectively, which allows naked-eye detection of fluoride ions.[10] When excited at 340 nm 416 nm and 330 nm respectively, the intensity of emission peaks of **1**, **2** and **3** decreased in the presence of fluoride (figure 10 and ESI Figure S15-S17). The changes associated with UV-Vis and PL features of **1** and **2** stops upon addition of one equivalent of TBAF while in the case of **3** saturation level reached after the addition of two equivalent of TBAF. This result confirms 1:1 complex (**1**+F^- and **2**+F^-) formation between **1** and **2** with fluoride and 1:2 complex (**3**+{**2F**}$^-$) formations between **3** with fluoride ions.

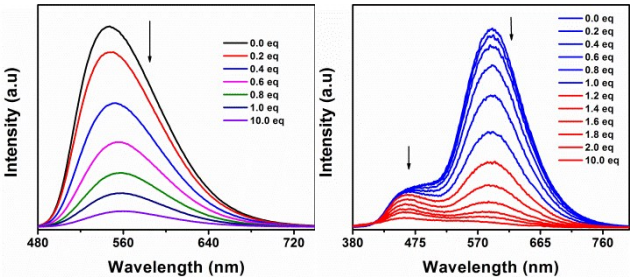

Figure 10: Changes in photoluminescence spectra of **2** (left) and **3** (right) (1 × 10^{-5} M) in presence of TBAF (2 μL = 1 eq) in dichloromethane.

Addition of CN^- ions to dichloromethane solutions of **1** gradually quenches the absorption bands at ~340 and 441 nm and the intensity of a new band at ~368 nm progressively increased. The spectral changes associated with **1** stop upon addition of two equivalents of cyanide ions. In the case of compounds **2** and **3**, two distinct changes were observed (Figure 11). First, until addition of 1.5 eq of CN, the absorption bands at ~ 340, ~420 and ~470 nm (slight blue shift was observed) with an isosbestic point at 375 nm. A new band at ~400 nm was also observed. Upon completion of 3 eq of CN ions, the intensity of all the absorption bands including the new absorption band at ~400 nm decrease. Further, a broad band in the region 280-340 nm evolved with a new isosbestic point at ~350 nm.

To get further insight into these binding events, the titrations were followed by ^{1}H NMR (ESI. Figure. S21-22). Addition of TBACN (tetra butyl ammonium cyanide) results in formation of multiple peaks in the aromatic region and two new singlets at ~4.25 and 4.36 ppm. The new resonance at 4.25ppm is typical of CN bound DCV unit.[14] Thus, the new resonance observed for compounds **1-3** in the presence of ~ 1 equivalent of TBACN can be ascribed to CN bound DCV units in these compounds. The appearance of new peak corresponding to CN-DCV units and the complex NMR pattern in the aromatic region clearly indicates that CN ions concomitantly binding to both the receptors TAB and DCV in compounds **1-3**. In the presence of 3 eq of TBACN, complex resonance pattern in the aromatic region become relatively simple. The resonance at ~4.36 ppm disappeared while the intensity of the signal corresponding to CN-DCV unit at ~4.25 ppm increased. This indicates that both receptors in **1-3** are saturated upon addition of 3 eq of CN. The fluoride binding event was also monitored by ^{1}H NMR studies. In the presence of 1 equivalent of fluoride ion, compounds showed complex ^{1}H resonance pattern in the region corresponding to mesityl groups. No changes in the DCV proton resonances were observed. In the presence of TBAF, ^{19}F NMR spectra of **1-3** showed a broad resonance at ~-171 ppm corresponding to $Ar_3B{\cdot}F^-$ complex (ESI). These results clearly suggest that F^- is binding only to boron centre.

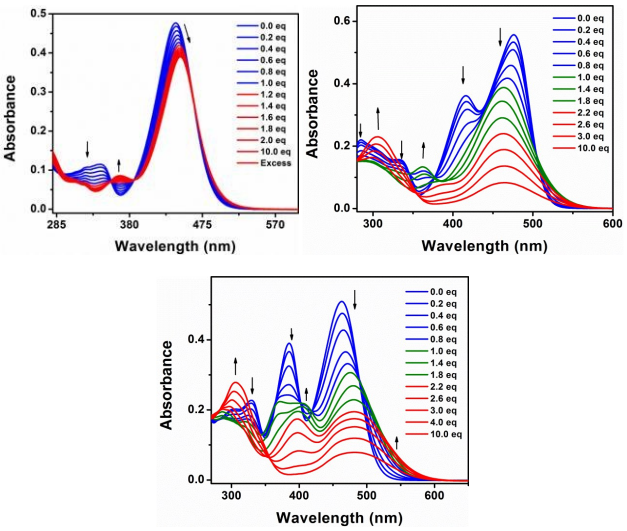

Figure 11: Changes in UV-Vis-absorption spectra of **1** (1 × 10^{-5} M, top left), **2** (1 × 10^{-5} M, top right), and **3** (1 × 10^{-5} M, bottom) in presence of TBACN (2 µL = 1 eq) in dichloromethane. The changes are almost similar to fluoride titration except the formation a new absorption band at ~370 nm. The band at 441 nm red shifted to 446 nm.

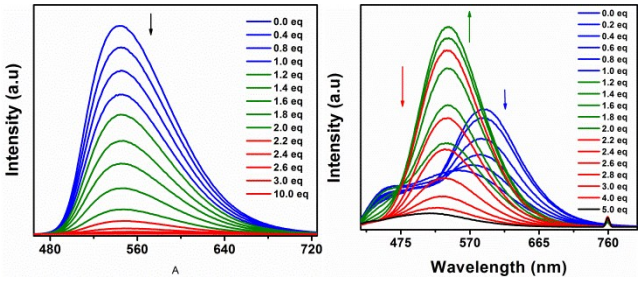

Figure 12: Changes in photoluminescence spectra of **2** (left) and **3** (right) (1 × 10^{-5} M) in presence of TBAF (2 µL = 1 eq) in dichloromethane.

In the case of **1** and **2**, cyanide binding quenches the fluorescence emission peaks at 481 nm and 546 nm respectively. Compound **3** showed intriguing PL spectral changes in the presence of cyanide ion (ESI, Figure S18-S20). Upon gradual addition of two equivalents of CN^- ions, the intensity of the fluorescence band at ~460 and ~ 592 nm decreases concurrently intensity of a new emission band at 540 nm gradually increased. Further addition of CN^- ions quenches the fluorescence peak at 540 nm and a residual emission was observed at 460 nm. The PL spectral changes stops upon addition 5 eq of CN ions.

Binding constants are calculated from UV-Vis absorption spectral changes (~ 340 nm) by the addition anion. The slope of Linear fitting of the plot $(1 - I/I_0)$/[Anion] Vs I/I_0 directly resulted the binding canstants (Table 3, Figure S28, S29) where I_0 and I are absorbance values at initial and at the presence of particular concentration of anion respectively. Compound **3** shows highest binding affinity towards fluoride/cyanide compared to both **1** and **2**, which can be due to the presence of two Lewis acidic boron centres.

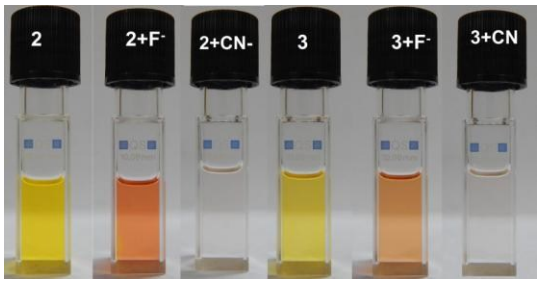

Figure 13: Photographs of **2** and **3** in the presence of fluoride and cyanide under daylight.

Reversible anion binding is very essential for probes to be applicable in practical purposes. In order to examine the reversibility of **1**, **2** and **3**, a Lewis acid $BF_3.OEt_2$ was used as an external reagent to extract the anions from fluoride complexes such as **1·F⁻**, **2·F⁻** and **3·{2F}⁻**. Addition of $BF_3{\cdot}OEt_2$ (~ 4×10^{-2} M, 2µL) to solutions of fluoride bound species (**1·F⁻**, **2·F⁻** and **3·{2F}⁻**) resulted in nearly complete restoration of luminescence of the respective free Lewis acidic probes **1**, **2** and **3** respectively (ESI, Figure S25). This result suggests compounds **1-3** bind with fluoride reversibly and can be reused. In the case of cyanide binding, CN^- binds with both the receptor centres (TAB and DCV).

Table 3: Binding constants

	1	2	3
K (F^-) (10^5 M^{-1})	0.19	1.01	2.43
K (CN^-) (10^5 M^{-1})	0.68	0.78	1.13

Binding constants are calculated from UV-Vis absorption titrations by plotting $(1 - I/I_0)$/[Anion] against I/I_0.For **1**, **2** and **3**, K value calculated for changes in absorption corresponds to TAB units.

Since, CN^- ions form a covalent bond with the electrophillic carbon centre of DCV unit, cyanide binding is not reversible at this receptor cite. However, the reversibility of TAB centre towards cyanide was monitored by using Fe^{3+} ions as an external reagent to remove boron bound CN^- ions from **1**·{2**CN**}$^-$, **2**·{2**CN**}$^-$ and **3**·{3**CN**}$^-$. In all the three cases, addition of Fe^{3+} ions (2.5×10^{-2} M, 2μL) increases the intensity of boryl based emission band at ~450 nm (ESI Figure S26). These observations indicate the reversible binding nature of TAB unit with cyanide ions.

To evaluate the sensitivity of the probes (**1**, **2** and **3**) towards fluoride and cyanide ions, detection limits are calculated by adopting the procedures reported elsewhere[6c, 15]. The changes in the fluorescence intensity of the probes **1-3** in the presence of various concentrations of F^-/CN^- ions (~1M to 10^{-10} M) was used to calculate the detection limits. The logarithmic value of anion concentration was plotted against $(I_{max} - I)/(I_{max} - I_{min})$ where I_{max}, I, and I_{min} are the initial fluorescence intensity, the intensity at a particular concentration, and the intensity at the saturation point, respectively. The intercept (ESI Figure S23 and S24) on the X-axis (here log[X^-]) was obtained by linear fitting of $(I_{max} - I)/(I_{max} - I_{min})$ versus log[X^-]. Detection limits are calculated by the formula {([X^-] × Mol.Wt of X)/1000 (multiplied by 10^6 to change the units to parts per million}, where X is TBAF or TBACN. Fluoride detection limits for compounds **1**, **2** and **3** are found to be ~2.1, ~0.82 and ~0.26 ppm respectively. In the case of cyanide ion, the detection limits were found as ~0.42, ~0.67 and ~0.21 ppm for **1**, **2** and **3** respectively. The observed limits of detections and binding constants clearly indicate that the reported molecules are highly sensitive for fluoride and cyanide ions.

Conclusions

In summary, modular design and synthesis of three new A – D - A (**1-3**) containing electron deficient dual receptors (TAB and DCV) is reported. The A-D-A structure of these sensors endowed two distinct ICT process in the visible region of the electronic spectra of **1-3**. All the compounds show high selectivity towards fluoride and cyanide ions. Particularly **2** and **3** shows unprecedented fluorogenic and colorimetric response towards interfering anions such as F^- and CN^-. The ^1H and ^{19}F NMR titration experiments revealed that fluoride ions bind only to boron centre while cyanide binds with both the receptor sites. The binding of F^-/CN^- induce colour changes in the visible region of the electronic spectra of **2** and **3**, which allows naked-eye detection of F^- and CN^- ions. We believe that this work opens a new pathway for the discrimination of two interfering anions by naked eye.

Experimental Section

Materials and Methods:

n-Butyllithium (1.6 M in hexanes) and Malanonitrile were purchased from Acros (india) and Spectrochem (India) respectively. All moisture sensitive reactions were carried under an atmosphere of purified Nitrogen using standard schlenck techniques. THF was distilled over sodium prior to use. HPLC grade solvents were used for absorption and emission spectroscopic measurements. All the UV-Vis absorption and fluorescence titrations are carried out at room temperature in freshly distilled solvents including NMR titrations. Absolute quantum yields are recorded using Integrating sphere. Single crystals suitable for X-ray diffraction[10] studies are obtained by slow evaporation of CH_2Cl_2 solutions of **2** at 25°C. The (400 MHz) ^1H NMR, (376 MHz) ^{19}F NMR, (100 MHz) ^{13}C NMR and (160 MHz) ^{11}B NMR were recorded on a Bruker Advance 400 MHz NMR spectrometer. Electronic absorption spectra were recorded on a Perkin Elmer LAMBDA 750 UV/visible spectrophotometer. Fluorescence emission and excitation spectra were recorded on a Horiba JOBIN YVON Fluoromax-4 spectrometer. Single-crystal X-ray diffraction studies were carried out with a Bruker SMART APEX diffractometer equipped with 3-axis goniometer.

Synthetic Procedures:

Compounds **2.1**, **3.1** and **4.1** are synthesized by reported literature methods[9].

Synthesis of B (4-((4-bromophenyl)(methyl)amino)benzaldehyde): To a solution of **A** (3 g, 8.79 mmol) in THF was added drop wise n-BuLi (1.6 M, 6.05 mL, 9.67 mmol) under N_2 atmosphere at -78 °C and stirred at this temperature for 60 min. To the reaction mixture was added DMF (xx mL, 26.37 mmol) and the reaction mixture was allowed to warm to room temperature and stirring continued. After 6 hr, 10 mL of 2N HCl was added and continued the stirring for another 4 h. After addition of water, the reaction mixture was extracted with ethyl acetate. The extract was washed with water, dried under Na_2SO_4 and concentrated under reduced pressure afforded crude product, which was further purified by silica gel column chromatography (petroleum ether/ EtOAc (96:4)). Yield: 1.8 g in 74.4% as dirty white solid. ^1H NMR (400 MHz, $CDCl_3$, δ ppm) 9.78 (s, 1H), 7.71 (d, *J* = 8 Hz, 2H), 7.54 (d, *J* = 8 Hz, 2H), 7.11 (d, *J* = 8 Hz, 2H), 6.81 (d, *J* = 8 Hz, 2H), 3.37 (s, 3H).

Synthesis of 1.1 (4-((4-(dimesitylboryl)phenyl)(methyl)amino)benzaldehyde): To a solution of **C** (1.8 g, 6.5 mmol) in ethanol (30 mL) was added triethylorthoformate (3.25 mL, 19.55 mmol) and catalytic amount of acid, and refluxed for 12 hours. Evaporation of all the volatiles under reduced pressure afforded **D** as yellowish liquid. Yield: 1.54 g in 67.54 %. ^1H NMR (400 MHz, $CDCl_3$, δ ppm). 7.38 (d, *J* = 8 Hz, 2H), 7.33 (d, *J* = 8 Hz, 2H), 7.02 (d, *J* = 8 Hz, 2H), 6.86 (d, *J* = 8 Hz, 2H), 5.47 (s, 1H), 3.65 (m, 3H), 3.54 (m, 3H), 3.30 (s, 3H), 1.25 (t, *J* = 8 Hz, 6H). To the solution of **D** (1.54 g, 4.23 mmol) in THF was added drop wise n-BuLi (1.6 M, 2.9 mL, 4.65 mmol) under N_2 atmosphere at -78 °C and stirred at this temperature for 60 min. To the reaction mixture was added $BFMes_2$ (1.25 g, 4.65 mmol) and the reaction mixture was allowed to warm to room temperature and stirring continued for another 12 hours. After addition of water,

the reaction mixture was extracted with ethyl acetate. The extract was washed with water, dried under Na_2SO_4 and concentrated under reduced pressure afforded crude product, which was further purified by silica gel column chromatography (petroleum ether/ EtOAc (96:4)). Yield: 0.4 g in 21.27 % as straw yellow solid. ^{1}H NMR (400 MHz, $CDCl_3$, δ ppm) 9.82 (s, 1H), 7.74 (d, *J* = 8 Hz, 2H), 7.53 (d, *J* = 8 Hz, 2H), 7.13 (d, *J* = 8 Hz, 2H), 7.02 (d, *J* = 8 Hz, 2H), 3.46 (s, 3H), 2.31 (s, 6H), 2.05 (s, 12H)

Synthesis of 1: 1.4 (0.1 g, 0.20 mmol) and malanonitrile (0.07 mL, 1.0 mmol) are taken in a mixture of DCM–ethanol (10 : 90). A catalytic amount of piperidine was added and the reaction mixture was stirred for one hour. Evaporation of all the volatiles gave the crude product which is further purified by silica gel column chromatography (hexane–ethylacetate 96:4). Yield: 0.05 g in 45.6 % as orange powder. ^{1}H NMR (400 MHz, $CDCl_3$, δ ppm) 7.79 (d, *J* = 8 Hz, 2H), 7.58 (d, *J* = 8 Hz, 2H), 7.51 (s, 1H), 7.18 (d, *J* = 8 Hz, 2H), 6.87 (d, *J* = 8 Hz, 2H), 3.48 (s, 3H), 2.32 (s, 6H), 2.04 (s, 12H). ^{13}C NMR (100 MHz, $CDCl_3$, δ ppm) 158.50, 153.62, 149.44, 141.22, 139.31, 138.79, 133.76, 128.74, 125.07, 122.05, 115.87, 115.47, 114.80, 74.96, 40.69, 23.94, 21.68. ESI mass calcl: $C_{35}H_{34}BN_3$ (M +Na^+) 530.2738. Found 530.2738.

Synthesis of 2: 2.1 (0.1 g, 0.182 mmol) and malanonitrile (0.029 mL, 0.45 mmol) are taken in a mixture of DCM–ethanol (10:90). A catalytic amount of piperidine was added and the reaction mixture was stirred for one hour. Evaporation of all the volatiles gave the crude product which is further purified by silica gel column chromatography (hexane–ethylacetate 96:4). Yield: 0.065 g in 55.5 % as red colour solid. ^{1}H NMR (400 MHz, $CDCl_3$, δ ppm) 7.86 (d, *J* = 8 Hz, 4H), 7.64 (s, 2H), 7.55 (d, *J* = 8 Hz, 2H), 7.19 (d, *J* = 10 Hz, 4H), 7.09 ((d, *J* = 8 Hz, 2H), 6.84 (s, 4H), 2.31 (s, 6H), 2.04 (s, 12H). ^{13}C NMR (100 MHz, $CDCl_3$, δ ppm) ESI mass calcl: $C_{44}H_{36}BN_5$ (M + Na^+) 668.6062. Found 668.6099.

Synthesis of 3: 3.1 (0.1 g, 0.123 mmol) and malanonitrile (0.021 mL, 0.325 mmol) are taken in a mixture of DCM–ethanol (10 : 90). A catalytic amount of piperidine was added and the reaction mixture was stirred for one hour. Evaporation of all the volatiles gave the crude product which is further purified by silica gel column chromatography (hexane–ethylacetate 96:4). Yield: 0.025 g in 23.5 % as reddish orange solid. ^{1}H NMR (400 MHz, $CDCl_3$, δ ppm). 7.80 (d, *J* = 8 Hz, 2H), 7.57 (s, 1H), 7.50 (d, *J* = 8 Hz, 4H), 7.12 (d, *J* = 10 Hz, 2H), 7.09 (d, *J* = 8 Hz, 4H), 6.83 (s, 8H), 2.31 (s, 12H), 2.05 (s, 24H). ^{13}C NMR (100 MHz, $CDCl_3$, δ ppm) 158.29, 152.77, 148.80, 143.63, 142.01, 141.21, 139.22, 138.63, 133.22, 128.72, 125.27, 122.05, 23.91, 21.66. ESI mass calcl: $C_{58}H_{57}B_2N_3$ (M + Na^+) 840.4631. Found 840.4631.

Acknowledgements

PT thanks the Department of Science and Technology (DST) New Delhi, and IISc, Bangalore for the financial support. GRK and SKS thank UGC New Delhi and IISc for research fellowships.

Notes and references

1 A. Sundararaman, K. Venkatasubbaiah, M. Victor, L. N. Zakharov, A. L. Rheingold, F. Jäkle, *J. Am. Chem. Soc.* 2006, **128**, 16554–16565. (b) Z. M. Hudson, S. Wang, *Accounts Chem. Res.* 2009, **42**, 1584–1596. (c) C.T. Poon, W. H. Lam, V. W.-W. Yam, *J. Am. Chem. Soc.* 2011, **133**, 19622–19625. (d) V. Zlojutro, Y. Sun, Z. M. Hudson, S. Wang, *Chem. Commun.* 2011, **47**, 3837-3839. (e) X. Liu, S. Li, J. Feng, Y. Li, G. Yang, *Chem. Commun*. 2014, **50**, 2778. (h) K. Matsuo, S. Saito, S. Yamaguchi, *J. Am. Chem. Soc.* 2014, **136**, 12580–12583. (f) T. Kushida, A. Shuto, M. Yoshio, T. Kato, S. Yamaguchi, *Angew. Chem. Int. Ed.* 2015, 54, 6922–6925. (g) V. M. Hertz, M. Bolte, H. W. Lerner, M. Wagner, *Angew. Chem. Int. Ed.* 2015, **54**, 8800-8804. (h) A. Hübner, T. Kaese, M. Diefenbach, B. Endeward, M. Bolte, H. W. Lerner, M. C. Holthausen, M. Wagner, *J. Am. Chem. Soc*. 2015, **137**, 3705−3714. (i) P. Joshi, R. Vedarajan and N. Matsumi, *Chem Commun*, **2015**, DOI: 10.1039/C5CC04753F.

2 (a) Y. Sun, N. Ross, S.-B. Zhao, K. Huszarik, W. L. Jia, R. Y. Wang, D. Macartney, S. Wang, *J. Am. Chem. Soc.* 2007, **129**, 7510–7511. (b) Z M. M. Hudson, S.-B. Zhao, R. Y. Wang, S. Wang, *Chem. Eur. J.* 2009, **15**, 6131–6137. (c) Y. Sun, S. Wang, *Inorg. Chem.* 2009, **48**, 3755–3767. (d) Z. M. Hudson, S. Wang, *Organometallics* 2011, **30**, 4695–4701. (e) Y. L. Rao, S. Wang, *Organometallics* 2011, **30**, 4453–4458. (f) Z. M. Hudson, S. Wang. *Dalton Trans.* 2011, **40**, 7805-7816. (g) Z. M. Hudson, M. G. Helander, Z. H. Lu, S. Wang, *Chem. Commun.* 2011, **47**, 755-757. (h) Y. L. Rao, D. Schoenmakers, Y. L. Chang, J. S. Lu, Z. H. Lu, Y. Kang, S. Wang, *Chem. Eur. J.* 2012, **18**, 11306–11316. (i) B. A. Blight, S. B. Ko, J.-S. Lu, L. F. Smith, S. Wang, *Dalton Trans.* 2013, **42**, 10089-10092. (j) X. Yang, Z. Huang, J. Dang, C. L. Ho, G. Zhou, W.-Y. Wong, *Chem. Commun.* 2013, **49**, 4406–4408. (k) S.-B. Ko, J.-S. Lu, Y. Kang, S. Wang, *Organometallics* 2013, **32**, 599–608. (l) H. Shi, D. Xin, X. Dong, J. Dai, X. Wu, Y. Miao, L. Fang, H. Wang, M. M. F. Choi, *J. Mater. Chem. C*, 2014, **2**, 2160-2168.

3 (a) Z. Q. Liu, Q. Fang, D. X. Cao, D. Wang, G. B. Xu, *Org. Lett.* 2004, **6**, 2933–2936. (b) Z. Yuan, C. D. Entwistle, J. C. Collings, D. Albesa-Jové, A. S. Batsanov, J. A. K. Howard, N. J. Taylor, H. M. Kaiser, D. E. Kaufmann, S.-Y. Poon, et al., *Chem. - Eur. J.* 2006, **12**, 2758–2771. (c) M. M. Alam, M. Chattopadhyaya, S. Chakrabarti, *Phys. Chem. Chem. Phys.* 2011, **13**, 9285-9292. (d) N. S. Makarov, S. Mukhopadhyay, K. Yesudas, J. L. Brédas, J. W. Perry , A. Pron, M. Kivala, K. Müllen, *J. Phys. Chem. A*, 2012, **116**, 3781–3793. (e) N. S. Makarov, S. Mukhopadhyay, K. Yesudas, J. Bredas, J. W. PerryJ, *Phys. Chem. A*, 2012, **116**, 3781−3793.

4 (a) Y. Qin, C. Pagba, P. Piotrowiak, F. Jäkle, *J. Am. Chem. Soc.* 2004, **126**, 7015–7018. (b) K. Parab, K. Venkatasubbaiah, F. Jäkle, *J. Am. Chem. Soc.* 2006, **128**, 12879–12885. (c) F. Jäkle, *Chem. Rev.* 2010, **110**, 3985–4022. (d) H. Li, F. Jäkle, *Macromol. Rapid Commun.* 2010, **31**, 915–920.

5 (a) S. Yamaguchi, S. Akiyama, K. Tamao, *J. Am. Chem. Soc.* 2001, **123**, 11372–11375. (b) Y. Kubo, M. Yamamoto, M. Ikeda, M. Takeuchi, S. Shinkai, S. Yamaguchi, K. Tamao, *Angew. Chem. Int. Ed.* 2003, **42**, 2036–2040. (c) Noriyoshi Matsumi, Masafumi Miyake and Hiroyuki Ohno, *Chem. Commun.*, 2004, 2852-2853 (d) C.-W. Chiu, F. P. Gabbaï, *J. Am. Chem. Soc.* 2006, **128**, 14248–14249. (e) D. R. Bai, X. Y. Liu, S. Wang, *Chem. Eur. J.* 2007, **13**, 5713–5723. (f) Q. Zhao, F. Li, S. Liu, M. Yu, Z. Liu, T. Yi, C. Huang, *Inorg. Chem.* 2008, **47**, 9256–9264. (g) A. Kawachi, A. Tani, J. Shimada, Y. Yamamoto, *J. Am. Chem. Soc.* 2008, **130**, 4222–4223. (h) T. W. Hudnall, Y.M. Kim, M. W. P. Bebbington, D. Bourissou, F. P. Gabbaï, *J. Am. Chem. Soc.* 2008, **130**, 10890–10891. (i) C. R. Wade, F. P. Gabbaï, *Dalton Trans.* 2009, 9169-9175. (j) T. Agou, M. Sekine, J. Kobayashi, T. Kawashima, *Chem.*

Commun. 2009, 1894-1896. (k) Z. M. Hudson, X. Y. Liu, S. Wang, *Org. Lett.* 2010, **13**, 300–303. (k) C. R. Wade, A. E. J. Broomsgrove, S. Aldridge, F. P. Gabbaï, *Chem. Rev.* 2010, **110**, 3958–3984. (l) Y. Kim, H.-S. Huh, M. H. Lee, I. L. Lenov, H. Zhao, F. P. Gabbaï, *Chem. Eur. J.* 2011, **17**, 2057–2062. (m) X. He, V. W. W. Yam, *Org. Lett.*, 2011, **13**, 2172–2175. (n) Z. Zhou, A. Wakamiya, T. Kushida, S. Yamaguchi, *J. Am. Chem. Soc.* 2012, **134**, 4529–4532. (o) T. Liu, Y. Yu, S. Chen, Y. Li, H. Liu, *RSC Adv.* 2013, **3**, 9973-9977. (p) C.T. Poon, W. H. Lam, H.L. Wong, V. W. W. Yam, *Chem. Eur. J.* 2014, **21**, 2182–2192. (q) M.N. Belzile, X. Wang, Z. M. Hudson, S. Wang, *Dalton Trans.* 2014, **43**, 13696-13703. (r) S. Sharma, H. Kim, Y. H. Lee, T. Kim, Y. S. Lee, M. H. Lee, *Inorg. Chem.* 2014, **53**, 8672–8680. (s) W. Lin, Q. Tan, H. Liang, K. Y. Zhang, S. Liu, R. Jiang, R. Hu, W. Xu, Q. Zhao, W. Huang, *J. Mater. Chem. C*, 2015, **3**, 1883-1887.

6 (a) C. A. P. Swamy, S. Mukherjee, P. Thilagar, *Chem. Commun.* 2013, **49**, 993–995. (b) S. K. Sarkar, S. Mukherjee, P. Thilagar, *Inorg. Chem.* 2014, **53**, 2343–2345. (c) C. A. P. Swamy, S. Mukherjee, P. Thilagar, *Inorg. Chem*. 2014, **53**, 4813-4823.

7 (a) J. Ma, P. K. Dasgupta, *Anal Chim Acta*. 2010, **2**, 117–125 (b) Y. H. Jeong, C. H. Lee, W. D. Jang, *Chem. Asian J*. 2012, **1**, 1562 – 1566. (b) Y. D. Lin, Y. S. Pen, W. Su, K. L. Liau, Y. S. Wen, C. H. Tu, C. H. Sun, T. J. Chow, *Chem. Asian J*. 2012, **7**, 2864 – 2871. (c) S. Madhu, M. Ravikanth, *Inorg. Chem.* 2014, **53**, 1646-1653. (d) N. Kumari, S. Jha, S. Bhattacharya, *Chem. Asian J*. 2014, **9**, 830 – 837, (e) I.S. Turan, E. U. Akkaya, *Org. Lett.*, 2014, **6**, 680–1683 (f) K. Kanagaraj, K. Pitchumani, *Chem. Asian J*. 2014, **9**, 146 – 152 (g) A. Dvivedi, P. Rajakannu, M. Ravikanth, *Dalton Trans*, 2015, **44**, 4054-4062.

8 (a) C. A. P. Swamy, S. Mukherjee, P. Thilagar, *Anal. Chem.* 2014, **86**, 3616-3624. (b) G. R. Kumar, P. Thilagar, *Dalton. Trans*, 2014, **43**, 7200-7207. (c) C. Wang, J. Jia, W. N. Zhang, H. Y. Zhang, C. H. Zhao, *Chem. Eur. J.* 2014, **20**, 16590–16601.

9 (a) S. Yamaguchi, T. Shirasaka, K. Tamao, *Org. Lett.* 2000, **2**, 4129–4132. (b) R. Stahl, C. Lambert, C. Kaiser, R. Wortmann, R. Jakober, *Chem. Eur. J.* 2006, **12**, 2358–2370. (c) T. Agou, J. Kobayashi, T. Kawashima, *Chem. Commun.* 2007, 3204-3206 (d) U. Megerle, F. Selmaier, C. Lambert, E. Riedle, S. Lochbrunner, *Phys. Chem. Chem. Phys.* 2008, **10**, 6245-6251. (e) T. Agou, M. Sekine, J. Kobayashi, T. Kawashima, *Chem. Commun.* 2009, 1894-1896. (f) Md. M. Alam, M. Chattopadhyaya. S. Chakrabarti, *Phys. Chem. Chem. Phys.* 2011, **13**, 9285-9292. (g) Z. M. Hudson, X. Y. Liu, S. Wang, *Org. Lett.* 2011, **13**, 300–303. (h) S. Zhang, Z. Qu, P. Tao, B. Brooks, Y. Shao, X. Chen, C. Liu, *J. Phys. Chem. C*, 2012, **116**, 12434–12442. (i) M. Mao, M.-G. Ren, Q. H. Song, *Chem. Eur. J.* 2012, **18**, 15512–15522 (j) M. Steeger, C. Lambert, *Chem. Eur. J.* 2012, **18**, 11937–11948. (k) X. Liu, Y. Zhang, He Li, Sigen A, H. Xia, Y. Mu, *RSC Adv.* 2013, **3**, 21267-21270. (l) W Zhao, X. Zhuang, D. Wu, F. Zhang, D. Gehrig, F. Laquai, X. Feng, *J. Mater. Chem. A*, 2013, **1**, 13878-13884. (m) M. N. Belzile, X. Wang, Z. M. Hudson, S. Wang, *Dalton Trans.* 2014, **43**, 13696-13703. (n) H. Shi, J. Yuan, X. Wu, X. Dong, L. Fang, Y. Miao, H. Wang, F. Cheng, *New J. Chem.* 2014, **38**, 2368-2378. (o) M. S. Yuan, Q. Wang, W. Wang, D. E. Wang, J. Wang, J. Wang, *Analyst*. 2014, **139**, 1541-1549. (p) Z. Zhang, R. M. Edkins, J. Nitsch, K. Fucke, A. Eichhorn, A. Steffen, Y. Wang, T. B. Marder, *Chem. Eur. J.* 2014, **21**, 177–190. (q) A. Ito, K. Kawanishi, E. Sakuda, N. Kitamura, *Chem. Eur. J.* 2014, **20**, 3940–3953. (r) A. G. Bonn, O. S. Wenger, *J. Org. Chem.* 2015, **80**, 4097–4107.

10 C. A. P. Swamy, P. Thilagar, *Inorg. Chem*, 2014, **53**, 2776-2876.

11 O. V. Dolomanov, L. J. Bourhis, R. J. Gildea, J. A. K. Howard, H. Puschmann, *J. Appl. Cryst.* 2009, **42**, 339-341.

12 E. Sakuda, Y. Ando, A. Ito, N. Kitamura, *J. Phys. Chem. A*, 2010, **114**, 9144;

13 (a) A. D. Becke, *J. Chem. Phys*, 1993, **98**, 5648. [b] M. J. Frisch, G. W. Trucks, H. B. Schlegel, G. E. Scuseria,M. A. Robb, J. R. Cheeseman, G. Scalmani, V. Barone,B. Mennucci, G. A. Petersson, H. Nakatsuji, M. Caricato,X. Li, H. P. Hratchian, A. F. Izmaylov, J. Bloino, G. Zheng,J. L. Sonnenberg, M. Hada, M. Ehara, K. Toyota, R. Fukuda,J. Hasegawa, M. Ishida, T. Nakajima, Y. Honda, O. Kitao,H. Nakai, T. Vreven, J. A. Montgomery, Jr., J. E. Peralta,F. Ogliaro, M. Bearpark, J. J. Heyd, E. Brothers, K. N. Kudin, V. N. Staroverov, R. Kobayashi, J. Normand, K. Raghavachari, A. Rendell, J. C. Burant, S. S. Iyengar,J. Tomasi, M. Cossi, N. Rega, J. M. Millam, M. Klene,J. E. Knox, J. B. Cross, V. Bakken, C. Adamo, J. Jaramillo,R. Gomperts, R. E. Stratmann, O. Yazyev, A. J. Austin,R. Cammi, C. Pomelli, J. W. Ochterski, R. L. Martin,K. Morokuma, V. G. Zakrzewski, G. A. Voth, P. Salvador,J. J. Dannenberg, S. Dapprich, A. D. Daniels, O. Farkas,J. B. Foresman, J. V. Ortiz, J. Cioslowski and D. J. Fox, *Gaussian 09, Revision A.02*, Gaussian, Inc., Wallingford CT, **2009**. (b) A. D. Becke, Phys. Rev. A: At., *Mo., Opt. Phys*, 1988, **38**, 3098.

14 (a) Z. Liu, X. Wang, Z. Yang, W. He, *J. Org. Chem.* 2011, **76**, 10286–10290. (b) X. Cheng, Y. Zhou, J. Qin, Zhen Li, *ACS Appl. Mater. Interfaces*, 2012, **4**, 2133–2138. (c) L. Yang, X. Li, J. Yang, Y. Qu, J. Hua, *ACS Appl. Mater. Interfaces*. 2013, **5**, 1317–1326. (d) W. C. Lin, S. K. Fang, J. Hu, H. Y. Tsai, Kew-Yu Chen, *Anal. Chem*, 2014, **86**, 4648-4652.

15 S. Anbu, S. Shanmugaraju, R. Ravishankaran, A. A. Karande, P. S. Mukherjee, *Inorganic Chemistry Communications*, 2012, **25**, 26–29.